Treatment of recalcitrant crystalline polysaccharides with lytic polysaccharide monooxygenase relieves the need for glycoside hydrolase processivity.

Anne Grethe Hamre, Anne-Grethe Skaarberg Strømnes, Daniel Gustavsen, Gustav Vaaje-Kolstad, Vincent G. H. Eijsink, and Morten Sørlie*

Department of Chemistry, Biotechnology and Food Science, Norwegian University of Life Sciences, PO 5003, N-1432 Ås, Norway.

* To whom correspondence should be addressed: Morten Sørlie (morten.sorlie@nmbu.no), Tel.: +47-67232562 and Fax: +47-64965901

Keywords: Processivity; glycoside hydrolase; lytic polysaccharide monooxygenase; recalcitrant polysaccharides

Abstract

Processive glycoside hydrolases associate with recalcitrant polysaccharides such as cellulose and chitin and repeatedly cleave glycosidic linkages without fully dissociating from the crystalline surface. The processive mechanism is efficient in the degradation of insoluble substrates, but comes at the cost of reduced enzyme speed. We show that less processive chitinase variants with reduced ability to degrade crystalline chitin, regain much of this ability when combined with a lytic polysaccharide monooxygenase (LPMO). When combined with an LPMO, several less processive chitinase mutants showed equal or even increased activity on chitin compared to the wild-type. Thus, LPMOs affect the need for processivity in polysaccharide degrading enzyme cocktails, which implies that the composition of such cocktails may need reconsideration.

1. Introduction

Chitin and cellulose represent some of nature's largest reservoirs of organic carbon in the form of monomeric hexose sugars (*N*-acetyl-glucosamine and glucose, respectively) linearly linked by β-1,4 glycosidic bonds. In their natural form, both polysaccharides are organized in crystalline arrangements that make up robust biological structures including crustacean cuticles (chitin) and plant cell walls (cellulose). Although these crystalline arrangements are crucial for biological function, they present a significant challenge in industrial utilization of biomass, where efficient enzymatic depolymerization is a critical step.

Enzymatic degradation of recalcitrant polysaccharides is thought to occur primarily through the synergistic action of glycoside hydrolases (GHs) that have complementary activities (Henrissat et al., 1985, Merino and Cherry, 2007). Endo-acting GHs make random scissions on the polysaccharide chains, whereas exo-acting GHs mainly target reducing and non-reducing chain ends. Both endo- and exo-acting GHs may be processive, which implies that they repeatedly cleave glycosidic linkages without fully dissociating from the crystalline surface. Lytic polysaccharide monooxygenases (LPMO) add to the degradation process by using a reduced oxygen species to cleave glycosidic bonds in crystalline regions, thus creating new chain ends for exo-acting GHs (Vaaje-Kolstad et al., 2010, Hamre et al., 2015a, Vaaje-Kolstad et al., 2005a, Harris et al., 2010). Processive GHs are typically the most abundant enzymes in both natural secretomes and industrial enzyme cocktails by virtue of their significant hydrolytic potential on crystalline substrates (Beckham et al., 2014). LPMOs also make considerable contributions to the overall efficiency of cellulolytic enzyme cocktails (Müller et al., 2015), but the interplay between LPMOs and individual (processive) GHs is not well understood.

Processive GHs have active site tunnels or deep clefts aligned with surface exposed aromatic amino acids that provide strong binding to the substrate (Rouvinen et al., 1990, Davies

and Henrissat, 1995, Varrot et al., 2003, Colussi et al., 2015, Hamre et al., 2015b, Hamre et al., 2017). Aromate-mediated carbohydrate recognition facilitates the necessary fluid binding to the crystalline polymers, increases the efficiency of substrate degradation, and may provide a necessary pushing potential to overcome substrate obstacles that otherwise could have led to stalling of the enzyme (Varrot et al., 2003, Horn et al., 2006, Zakariassen et al., 2009, Hamre et al., 2014, Kuusk et al., 2015, Kurašin et al., 2015, Igarashi et al., 2011). The cost of the processive mechanism is loss of enzyme speed as the required strong interactions make the enzymes intrinsically slow. Indeed, studies of processive chitinases (Horn et al., 2006, Zakariassen et al., 2009) have shown that replacement of aromatic amino acids by alanine led to reduced processivity and decreased activity on crystalline chitin, while yielding an up to 30-fold increase in the rate of hydrolysis of water soluble chitosan. A consequence is that, in some cases, it might be better to focus strategies for enzymatic depolymerization of polysaccharide biomass on improving substrate accessibility for non-processive enzymes rather than on improving the properties of processive enzymes (Horn et al., 2006). Such strategies could include the use of LPMOs, which are known to disrupt the crystalline structure of chitin and cellulose (Vaaje-Kolstad et al., 2010, Villares et al., 2017, Song et al., 2018, Eibinger et al., 2014).

In this work, we have investigated how treatment with a chitin-active LPMO affects the initial rate of chitin hydrolysis by engineered variants of two exo-processive chitinases from *Serratia marcescens* with different degrees of processivity. The results show that the LPMO makes the crystalline material more amenable to the action of chitinase variants with reduced processivity, and have potential implications for the future design of enzyme cocktails for conversion of recalcitrant polysaccharides.

2. Materials and methods

2.1 Chemicals

Chito-oligosaccharides (CHOS) were purchased from Megazyme (Wicklow, Ireland). Squid pen *β*-chitin was purchased from France Chitine (180 μm microparticulate, Marseille, France). All other chemicals were of analytical grade and purchased from standard manufacturers.

2.2 Site-directed mutagenesis

Most chitinase variants used in this study have been described previously. Variants *Sm*ChiB-F190A and *Sm*ChiB-F190A/W220A (using *Sm*ChiB-WT and *Sm*ChiB-F190A as template, respectively) were generated using the QuikChange site directed mutagenesis kit from Stratagene (La Jolla, CA, USA), mainly as described by the manufacturer. The primers used for the mutagenesis are listed in Table 1 and were purchased from Life Technologies (Carlsbad, CA, USA). To confirm that the gene contained the desired mutation and to check for the occurrence of non-desirable mutations, the mutated genes were sequenced using the LIGHTrun sequencing service of GATC Biotech (Constance, Germany), before they were transformed into *Escherichia coli* BL21Star (DE3) cells (Life Technologies).

2.3 Protein expression and purification

The chitinases were from *S. marcescens* strain BJL200 (Brurberg et al., 1994, Brurberg et al., 1995). *Sm*ChiA-WT, *Sm*ChiB-WT, *Sm*ChiA-W167A, *Sm*ChiA-W275A, *Sm*ChiB-W97A, *Sm*ChiB-W220A, *Sm*ChiB-W97A/W220A, and *Sm*ChiB-F190A were expressed in *E. coli* as described previously (Brurberg et al., 1996) (Zakariassen et al., 2009, Horn et al., 2006). The same applies for *Sm*LPMO10A (previously known as CBP21) (Vaaje-Kolstad et al., 2005b). The periplasmic extracts were loaded on a column packed with chitin beads (New England

Biolabs, Ipswich, MA, USA) equilibrated in 50 mM Tris-HCl pH 8.0 (chitinases) or 50 Mm Tris-HCl pH 8.0, 1 M ammonium sulfate (*Sm*LPMO10A)After washing the column with the same buffer, the enzymes were eluted with 20 mM acetic acid. Purified proteins were further concentrated by use of Macrosep® Advances Centrifugal Devices (PALL Corporation, New York, NY) with a molecular mass cutoff of 30000 Da (chitinases) or Amicon Ultra Centrifugal filters (Merck Millipore, Darmstadt, Germany) with a molecular mass cutoff of 10000 Da (*Sm*LPMO10A). The chitinases and *Sm*LPMO10A were stored at 4 °C in 100 mM Tris-HCl pH 8.0 or 50 mM sodium acetate buffer pH 6.1, respectively.

The *Sm*ChiB-F190A/W220A gene was expressed as described previously for wild type *Sm*ChiB and its mutants (Brurberg et al., 1995, Horn et al., 2006). The periplasmic extract was adjusted to Buffer A (50 mM Tris-HCl pH 8.0, 1 M $(NH_4)_2SO_4$) with 3M $(NH_4)_2SO_4$ and loaded onto a HiTrap PhenyL HP column (5 mL) (GE Healthcare, Little Chalfont, Great Britain) connected to a BioLogic low-pressure protein purification system (Bio-Rad, Hercules, CA, USA). The chitinase was eluted by applying a two-step gradient where the first step was a linear salt gradient from 100 % buffer A to 70 % buffer B (50 mM Tris-HCl pH 8.0) over 10 column volumes at a flow rate of 4 ml/min. The second step was a new linear salt gradient from 70 – 100 % buffer B over 15 column volumes at a flow rate of 4 ml/min. Finally, buffer B was applied for 5 column volumes. The chitinase containing fractions were detected by SDS-PAGE, pooled and concentrated to 1 ml, using Macrosep® Advances Centrifugal Devices (PALL Corporation) with a molecular mass cutoff of 30000 Da. Subsequently, samples were loaded onto a HiLoad 16/600 Superdex 75 Prepgrade column (GE Healthcare), with a running buffer consisting of 20 mM Tris-HCl pH 8.0 and 0.2 M NaCl, using a flow rate of 1 ml/min. The chitinase eluted approximately 60 minutes after injection. The buffer was changed to 100 mM Tris-HCl pH 8.0 using Macrosep® Advances Centrifugal Devices (30000 Da cutoff) (PALL Corporation).

For all enzymes, chitinases and *Sm*LPMO10A, enzyme purity was verified by SDS-PAGE and the enzyme concentration was estimated by using the Bradford Protein Assay from Bio-Rad.

2.4 Time course of chitin degradation

Hydrolysis of chitin (20 mg/ml) was carried out in 50 mM sodium acetate at pH 6.1. Previously, we have shown that 20 mg/ml chitin gives substrate saturating conditions (Hamre et al., 2015a). The chitin samples were sonicated for 20 min in a sonication bath (Transonic Elma) to increase the surface of the substrate and thereby increase the availability of chitin ends for the enzymes (Fan et al., 2008). The reaction tubes were incubated at 37 °C in an Eppendorf thermomixer at 800 rpm. The chitinase concentration was 100 nM in all experiments. Aliquots of 75 µl were withdrawn every hour for 7 hours, and the enzymes were inactivated by adding 75 µl 20 mM H_2SO_4. Prior to further HPLC analysis all samples were filtrated through a 0.45 µm Duapore membrane (Merck Millipore) to remove denatured protein and chitin particles. All reactions were run in, at least, triplicate, and all samples were stored at –20 °C until HPLC analysis.

*2.5 Time course of chitin degradation after treatment with Sm*LPMO10A

The degradation was carried out as described in section 2.4 with the following exception: After sonication, *Sm*LPMO10A and ascorbic acid were added to an end concentration of 1 µM and 2 mM, respectively. The samples were incubated at 37 °C in an Eppendorf thermomixer at 800 rpm for 2.5 h before the addition of chitinase.

2.6 Determination of apparent degree of processivity

In this work, apparent degree of processivity was was assessed on the basis of the initial [$(GlcNAc)_2$]/[GlcNAc] product ratio from chitin hydrolysis as described in Hamre *et al*. (Hamre et al., 2014). Hydrolysis of chitin (2.0 mg/ml) was carried out in 50 mM sodium acetate buffer at pH 6.1. The chitin samples were sonicated for 20 min in a sonication bath (Transsonic, Elma). The reaction tubes were then incubated at 37 °C in an Eppendorf thermomixer at 800 rpm to avoid settling of the chitin particles. The chitinase concentration was 2.5 μM. Aliquots of 75 μL were withdrawn at regular time intervals, and the enzymes were inactivated by adding 75 μL 20 mM H_2SO_4. Prior to further HPLC analysis all samples were filtrated through a 0.45 μm Duapore membrane (Merck Millipore) to remove denatured protein and chitin particles. All reactions were performed in duplicate, and all samples were stored at –20 °C until HPLC analysis.

2.7 High performance liquid chromatography (HPLC)

Concentrations of mono- and disaccharides were determined using a Dionex Ultimate 3000 UHPLC system (Dionex Corp., Sunnyvale, CA, USA) equipped with a Rezex Fast fruit H^+ column (100 mm length and 7.8 mm inner diameter) (Phenomenex, Torrance, CA, USA). The sample size was 8 μl, and the mono- and disaccharides were eluted isocratically at 1 mL/min with 5 mM H_2SO_4 at 85 °C. The mono- and disaccharides were monitored by measuring absorbance at 195 nm, and the amounts were quantified by measuring peak areas. Peak areas were compared with peak areas obtained with standard samples with known concentrations of mono- and disaccharides. The degree of degradation (in percent) is defined as the amount of solubilized GlcNAc units divided by the amount of GlcNAc units in the chitin polymer at the start of the experiment.

2.8 Determination of A- and b-values for activity

According to Kostylev and Wilson, the following two-parameter kinetic model can be used to determine a time-dependent activity constant for polysaccharide degradation by a glygoside hydrolase:

$$X = At^b \quad (1)$$

where t is time (h), X is degree of degradation (in percent) is defined as the amount of solubilized GlcNAc units divided by the amount of GlcNAc units in the chitin polymer at the start of the experiment, A is the activity of the added enzyme, and b is an intrinsic constant that quantifies the curvature of the time course profile (Kostylev and Wilson, 2013). A and b values were determined after fitting the data from chitin degradation reactions to equation 1 by use of Origin Pro 7.5 Software.

3. Results and discussion

Serratia marcescens is a soil bacterium that produces four chitin-depolymerizing enzymes: *Sm*ChiC, an endo-nonprocessive chitinase, *Sm*ChiA and *Sm*ChiB, two exo-processive chitinases moving along chitin chains in opposite directions, and *Sm*LPMO10A, a surface-active lytic polysaccharide monooxygenase, also known as CBP21, that introduces chain breaks by oxidative cleavage (Vaaje-Kolstad et al., 2013). Previous studies have shown that aromatic amino acids in so-called substrate binding subsites, i.e. subsites interacting with the polymeric part of the chitin chain during processive action, are crucial for the processive ability of *Sm*ChiA and *Sm*ChiB (Horn et al., 2006, Zakariassen et al., 2009).

In *Sm*ChiB, residues important for processivity include Trp^{97} (subsite +1), Trp^{220} (subsite +2), and Phe^{190} (subsite +3) (Figure 1). In *Sm*ChiA, Trp^{167} in the substrate-binding subsite –3 is crucial for processivity, while processivity is also affected, albeit to a lesser extent byTrp^{275} and Phe^{396} in product binding subsites +1 and +2, respectively, where dimeric products are

released during processive hydrolysis (Zakariassen et al., 2009). Processivity implies that upon hydrolysis and release of the dimeric product the enzyme has a larger change of rebinding compared to diffusing away from the remaining substrate and the impact of the product binding subsites in *Sm*ChiA is likely due to promoting rebinding (Zakariassen et al., 2009, Kurašin et al., 2015).

Experimental assessment of processivity may be done using several methods but is not straightforward (see Horn *et al*. for further discussion, (Horn et al., 2012)). The apparent processive ability (P^{app}) provides a quantitative parameter and is defined as the average number of catalytic acts that an enzyme performs per one initiation of a processive run, which may be derived from various types of experiments, each with potential limitations. In Figure 2, we have illustated how P^{app} can be determined from determination of the ratio of dimeric products vs. monomeric products, which is a "classical" method for processive GH action and used to for *Sm*ChiB-F190A in this study (Horn et al., 2012). Regardless of these limitations, especially when it comes to quantification, available previous and newly generated data (Table 2) clearly show that all single mutants used in this study exhibit reduced processivity compared to the wild types.

Assessing kinetics of GH catalyzed hydrolysis of recalcitrant polysaccharides are not trivial (Bansal et al., 2009). It is very common to observe nonlinear behavior at a low degree of substrate conversion (Kostylev and Wilson, 2013, Kuusk et al., 2015). Different enzyme- and substrate-related factors can be responsible for the rapid decrease in hydrolysis rates such as the substrate being heterogeneous resulting in different parts being degraded faster than others, and that GHs tend to get stuck on the surface (Igarashi et al., 2011, Kurašin and Väljamäe, 2011, Bansal et al., 2009). Kostylev and Wilson have developed a simple two-parameter equation (Equation 1) to tackle this. One of the parameters is a total activity coefficient and the other is an intrinsic constant that reflects the ability of the GHs to overcome the varying degree of

substrate recalcitrance. This properly addresses the observed nonlinearities and allows for the direct comparison between different GH actions on the same substrate (Kostylev and Wilson, 2013). Since all wild types and mutated variants showed nonlinear rates in the presences of *Sm*LPMO10A, we opted to use Equation 1 in our kinetic analysis. It is proposed that LPMO action create new chain ends, and by this will increase the heterogeneity of the substrate. All *Sm*ChiB mutated variants showed activities (A values) amounting to approximately 15 % of the wild type activity (Table 2 and Fig. 3). As expected, the addition of *Sm*LPMO10A resulted in an increase (13-fold) in *Sm*ChiB activity. Remarkably, the effect of *Sm*LPMO10A on less processive *Sm*ChiB variants was much more pronounced. For example, the activity of *Sm*ChiB-W97A was increased 55-fold and in the presence of *Sm*LPMO10A the activity was 65 % of the wild type, as opposed to 16 % in the absence of *Sm*LPMO10A. Likewise, addition of *Sm*LPMO10A yielded a 68-fold increase in the activity of *Sm*ChiB-F190A and the activity was equal to that of the wild type enzyme. Interestingly, chitin hydrolysis by *Sm*ChiB-W220A became 160-fold faster in the presence of *Sm*LPMO10A making this mutant 1.55-fold more active than the wild type enzyme. In the presence of *Sm*LPMO10A, each of the double mutants displayed activities similar to the wild type enzyme.

Interestingly, the presentence of *Sm*LPMO10A resulted in less activation of *Sm*ChiA compared to ChiB (7-fold vs. 13-fold), in line with previous results (Hamre et al., 2015a). Also for *Sm*ChiA, the presence of *Sm*LPMO10A caused rate enhancements for the less processive mutants that were larger compared to the wild-type, but to a lesser degree than for the *Sm*ChiB mutants (30- and 12-fold increase for *Sm*ChiA-W167A and *Sm*ChiA-275A, respectively). Furthermore, in the presence of *Sm*LPMO10A the activities of the less processive mutants only reached 66 % and 48 %, respectively, of the wild type activity (as compared to up to 155 % for *Sm*ChiB-W220A).

From these results, it is clear that the need for processivity in enzymatic degradation of polysaccharides may be reduced when the crystalline substrate is treated with an LPMO. The trends are the same for all less processive variants, but the clearest example is provided by *Sm*ChiB-W220A, which in reactions with *Sm*LPMO10A displayed a 55 % increase in activity compared to the wild type under identical conditions. Crystallographic studies (Figure 1) show that Trp^{220} interacts closely with the substrate, thus likely making a major contribution to keeping the enzyme closely associated to the substrate in between subsequent hydrolytic reactions and preventing once-detached single chains from re-associating with the insoluble material (Teeri, 1997, Horn et al., 2006). Having access to numerous new chain ends provided by the LPMO liekly reduces the beneficial effect of the "stickiness" provided by Trp220 (and other aromatic ressidues near the catalytic center). This reasoning is in line with the notion that the rate-determining step for chitinase catalyzed hydrolysis changes from substrate association, for chitin, to product displacement when the substrate becomes more available as in the soluble chitin variant chitosan (Zakariassen et al., 2010).

It has been shown that Trp^{97} (subsite +1) and Phe^{190} (subsite +3) provide less binding free energy compared to Trp^{220} (Hamre et al., 2017, Jana et al., 2016). Moreover, While Trp^{220} seems only involved in substrate-binding and seems pre-ordered to do so in the apo-enzyme, Trp^{97} has an additional catalytic role since it takes part in stabilizing the energetically demanding $^{4}C_{1}$ to $^{1,4}B$ conformational change of the *N*-acetylglucosamine in the -1 subsite (Biarnes et al., 2007, van Aalten et al., 2001). Phe^{190} shows a -91° rotation around χ_1 upon substrate binding (van Aalten et al., 2001), which may slightly offset the benefical effect of the Phe-substrate interaction. These differences may underly the observed variations in the rate enhancements observed upon adding *Sm*LPMO10A.

Previous studies have shown that the initial rate of endo-nonprocessive *Sm*ChiC of *S. marcescens* is not enhanced by treatment with an LPMO, in line with the proposed main role

of LPMOs to create new chain-ends for exo-acting GHs (Hamre et al., 2015a). To this regard, it is interesting to observe that the rate of hydrolysis is more enhanced for *Sm*ChiB than for *Sm*ChiA. It has been suggested that, when acting on chitin, *Sm*ChiA is the most endo-active of the two GHs (Brurberg et al., 1996). Moreover, the mutation of either Trp^{167} or Trp^{275} to Ala, changes the probability of endo mode-initiation of hydrolysis by *Sm*ChiA from 76 % to 90 % (Kurašin et al., 2015). The increase in endo mode-initiation is one possible cause of the observed lower effect of *Sm*LPMO10A on the efficiency of the *Sm*ChiA mutants compared to the *Sm*ChiB mutants.

The advent of LPMOs has already led to considerable improvements of enzyme cocktails for biomass processing (Müller et al., 2015, Johansen, 2016), while recent results related to the nature of the co-substrate (O_2 or H_2O_2) and enzyme stability suggest that the potential of LPMOs has not yet been fully harnessed (Bissaro et al., 2017, Müller et al., 2018, Kuusk et al., 2018). So far, the interplay between LPMOs and individual GHs with varying functionalities (endo-, exo, processive) has not been studies in much detail. The present data show that the inclusion of LPMOs in enzyme cocktails may affect the need for certain GH types, in this case the highly "sticky" exoprocessive enzymes often referred to as chito- or cello-biohydrolases. Thus, harnessing the full potential of LPMOs not only requires selection of the best LPMOs and LPMO-friendly processing conditions, but also a reconsideration of the glycoside hydrolase composition of polysaccharide degrading enzyme cocktails.

ACKNOWLEDGMENTS

This work was supported by grants from the Norwegian Research Council 209335 (MS)

Reference List

BANSAL, P., HALL, M., REALFF, M. J., LEE, J. H. & BOMMARIUS, A. S. 2009. Modeling cellulase kinetics on lignocellulosic substrates. *Biotechnol. Adv.,* 27**,** 833-848.

BECKHAM, G. T., STÅHLBERG, J., KNOTT, B. C., HIMMEL, M. E., CROWLEY, M. F., SANDGREN, M., SØRLIE, M. & PAYNE, C. M. 2014. Towards a molecular-level theory of carbohydrate processivity in glycoside hydrolases. *Curr. Opin. Struct. Biol.,* 27**,** 96-106.

BIARNES, X., ARDEVOL, A., PLANAS, A., ROVIRA, C., LAIO, A. & PARRINELLO, M. 2007. The conformational free energy landscape of *ƒ*-D-glucopyranose. Implications for substrate preactivation in *ƒ*-glucoside hydrolases. *J. Am. Chem. Soc.,* 129**,** 10686-10693.

BISSARO, B., RØHR, A. K., SKAUGEN, M., FORSBERG, Z., HORN, S. J., VAAJE-KOLSTAD, G. & EIJSINK, V. G. H. 2017. Oxidative cleavage of polysaccharides by monocopper enzymes depends on H2O2. *Nat. Chem. Biol.,* 13**,** 1123-1128.

BRURBERG, M. B., EIJSINK, V. G., HAANDRIKMAN, A. J., VENEMA, G. & NES, I. F. 1995. Chitinase B from *Serratia marcescens* BJL200 is exported to the periplasm without processing. *Microbiology,* 141 (Pt 1)**,** 123-131.

BRURBERG, M. B., EIJSINK, V. G. & NES, I. F. 1994. Characterization of a chitinase gene (chiA) from *Serratia marcescens* BJL200 and one-step purification of the gene product. *FEMS Microbiol. Lett.,* 124**,** 399-404.

BRURBERG, M. B., NES, I. F. & EIJSINK, V. G. H. 1996. Comparative studies of chitinases A and B from Serratia marcescens. *Microbiology,* 142**,** 1581-1589.

COLUSSI, F., SØRENSEN, T. H., ALASEPP, K., KARI, J., CRUYS-BAGGER, N., WINDAHL, M. S., OLSEN, J. P., BORCH, K. & WESTH, P. 2015. Probing Substrate Interactions in the Active Tunnel of a Catalytically Deficient Cellobiohydrolase (Cel7). *J. Biol. Chem.,* 290**,** 2444-2454.

DAVIES, G. J. & HENRISSAT, B. 1995. Structures and Mechanisms of Glycosyl Hydrolases. *Structure,* 3**,** 853-859.

EIBINGER, M., GANNER, T., BUBNER, P., ROŠKER, S., KRACHER, D., HALTRICH, D., LUDWIG, R., PLANK, H. & NIDETZKY, B. 2014. Cellulose surface degradation by a lytic polysaccharide monooxygenase and Its effect on cellulase hydrolytic efficiency. *J. Biol. Chem.,* 289**,** 35929-35938.

FAN, Y., SAITO, T. & ISOGAI, A. 2008. Preparation of chitin nanofibers from squid pen *β*-chitin by simple mechanical treatment under acid conditions. *Biomacromolecules,* 9**,** 1919-1923.

HAMRE, A. G., EIDE, K. B., WOLD, H. H. & SØRLIE, M. 2015a. Activation of enzymatic chitin degradation by a lytic polysaccharide monooxygenase. *Carbohydr. Res.,* 407**,** 166-169.

HAMRE, A. G., FRØBERG, E. E., EIJSINK, V. G. H. & SØRLIE, M. 2017. Thermodynamics of Tunnel Formation upon Substrate Binding in a Processive Glycoside Hydrolase. *Arch. Biochem. Biophys.,* 620**,** 35-42.

HAMRE, A. G., JANA, S., HOLEN, M. M., MATHIESEN, G., P., V., PAYNE, C. M. & SØRLIE, M. 2015b. Thermodynamic Relationships with Processivity in *Serratia Marcescens* Family 18 Chitinases. *J. Phys. Chem. B,* 119**,** 9601-9613.

HAMRE, A. G., LORENTZEN, S. B., VÄLJAMÄE, P. & SØRLIE, M. 2014. Enzyme Processivity changes with the Extent of Recalcitrant Polysaccharide Degradation. *FEBS Lett.,* 588**,** 4620-4624.

HARRIS, P. V., WELNER, D., MCFARLAND, K. C., RE, E., NAVARRO POULSEN, J. C., BROWN, K., SALBO, R., DING, H., VLASENKO, E., MERINO, S., XU, F., CHERRY, J., LARSEN, S. & LO LEGGIO, L. 2010. Stimulation of lignocellulosic biomass hydrolysis by proteins of glycoside hydrolase family 61: Structure and function of a large, enigmatic family. *Biochemistry,* 49**,** 3305-3316.

HENRISSAT, B., DRIGUEZ, H., VIET, C. & SCHULEIN, M. 1985. Synergism of cellulases from *Trichoderma reesei* in the degradation of cellulose. *Bio-Technology,* 3**,** 722-726.

HORN, S. J., SIKORSKI, P., CEDERKVIST, J. B., VAAJE-KOLSTAD, G., SØRLIE, M., SYNSTAD, B., VRIEND, G., VÅRUM, K. M. & EIJSINK, V. G. H. 2006. Costs and Benefits of Processivity in Enzymatic Degradation of Recalcitrant Polysaccharides. *Proc. Natl. Acad. Sci. U.S.A.,* 103**,** 18089-18094.

HORN, S. J., SØRLIE, M., VÅRUM, K. M., VÄLJAMÄE, P. & EIJSINK, V. G. H. 2012. Measuring Processivity. *Meth. Enzymol.*: Academic Press.

IGARASHI, K., UCHIHASHI, T., KOIVULA, A., WADA, M., KIMURA, S., OKAMOTO, T., PENTTILÄ, M., ANDO, T. & SAMEJIMA, M. 2011. Traffic Jams reduce Hydrolytic Efficiency of Cellulase on Cellulose Surface. *Science,* 333**,** 1279-1282.

JANA, S., HAMRE, A. G., WILDBERGER, P., HOLEN, M. M., EIJSINK, V. G. H., BECKHAM, G. T., SØRLIE, M. & PAYNE, C. M. 2016. Aromatic-mediated Carbohydrate Recognition in Processive *Serratia Marcescens* Chitinases. *J. Phys. Chem. B,* 120**,** 1236-1249.

JOHANSEN, K. S. 2016. Discovery and industrial applications of lytic polysaccharide mono-oxygenases. *Biochem. Soc. Trans.,* 44**,** 143-149.

KOSTYLEV, M. & WILSON, D. 2013. Two-Parameter Kinetic Model Based on a Time-Dependent Activity Coefficient Accurately Describes Enzymatic Cellulose Digestion. *Biochemistry,* 52**,** 5656-5664.

KURAŠIN, M., KUUSK, S., KUUSK, P., SØRLIE, M. & VÄLJAMÄE, P. 2015. Slow Off-rates and Strong Product Binding are Required for Processivity and Efficient Degradation of Recalcitrant Chitin by Family 18 Chitinases. *J. Biol. Chem.,* 290**,** 29074-29085.

KURAŠIN, M. & VÄLJAMÄE, P. 2011. Processivity of Cellobiohydrolases is Limited by the Substrate. *J. Biol. Chem.,* 286**,** 169-177.

KUUSK, S., BISSARO, B., KUUSK, P., FORSBERG, Z., EIJSINK, V. G. H., SØRLIE, M. & VÄLJAMÄE, P. 2018. Kinetics of H2O2-driven degradation of chitin by a bacterial lytic polysaccharide monooxygenase. *J. Biol. Chem.,* 293**,** 523-531.

KUUSK, S., SØRLIE, M. & VÄLJAMÄE, P. 2015. The predominant molecular state of bound enzyme determines the strength and type of product inhibition in the hydrolysis of recalcitrant polysaccharides by processive enzymes. *J. Biol. Chem.*

MERINO, S. T. & CHERRY, J. 2007. Progress and challenges in enzyme development for biomass utilization. *Adv. Biochem. Eng. Biotechnol.,* 108**,** 95-120.

MÜLLER, G., CHYLENSKI, P., BISSARO, B., EIJSINK, V. G. H. & HORN, S. J. 2018. The impact of hydrogen peroxide supply on LPMO activity and overall saccharification efficiency of a commercial cellulase cocktail. *Biotechnol. Biofuels,* 11**,** 209.

MÜLLER, G., VÁRNAI, A., JOHANSEN, K. S., EIJSINK, V. G. H. & HORN, S. J. 2015. Harnessing the potential of LPMO-containing cellulase cocktails poses new demands on processing conditions. *Biotechnol. Biofuels,* 8**,** 187.

PAPANIKOLAU, Y., PRAG, G., TAVLAS, G., VORGIAS, C. E., OPPENHEIM, A. B. & PETRATOS, K. 2001. High resolution structural analyses of mutant chitinase A complexes with substrates provide new insight into the mechanism of catalysis. *Biochemistry,* 40**,** 11338-11343.

ROUVINEN, J., BERGFORS, T., TEERI, T., KNOWLES, J. K. & JONES, T. A. 1990. Three-dimensional structure of cellobiohydrolase II from Trichoderma reesei. *Science,* 249**,** 380-6.

SONG, B., LI, B., WANG, X., SHEN, W., PARK, S., COLLINGS, C., FENG, A., SMITH, S. J., WALTON, J. D. & DING, S.-Y. 2018. Real-time imaging reveals that lytic polysaccharide monooxygenase promotes cellulase activity by increasing cellulose accessibility. *Biotechnol. Biofuels,* 11**,** 41.

TEERI, T. T. 1997. Crystalline Cellulose Degradation: New Insight into the Function of Cellobiohydrolases. *Trends Biotechnol.,* 15**,** 160-167.

VAN AALTEN, D. M. F., KOMANDER, D., SYNSTAD, B., GÅSEIDNES, S., PETER, M. G. & EIJSINK, V. G. H. 2001. Structural insights into the catalytic mechanism of a family 18 exo-chitinase. *Proc. Natl. Acad. Sci. U.S.A,* 98**,** 8979-8984.

VARROT, A., FRANDSEN, T. P., VON OSSOWSKI, I., BOYER, V., COTTAZ, S., DRIGUEZ, H., SCHULEIN, M. & DAVIES, G. J. 2003. Structural Basis for Ligand Binding and Processivity in Cellobiohydrolase Cel6A from *Humicola Insolens*. *Structure,* 11**,** 855-864.

VILLARES, A., MOREAU, C., BENNATI-GRANIER, C., GARAJOVA, S., FOUCAT, L., FALOURD, X., SAAKE, B., BERRIN, J.-G. & CATHALA, B. 2017. Lytic polysaccharide monooxygenases disrupt the cellulose fibers structure. *Sci. Rep.,* 7**,** 40262.

VAAJE-KOLSTAD, G., HORN, S. J., SØRLIE, M. & EIJSINK, V. G. H. 2013. The chitinolytic machinery of Serratia marcescens – a model system for enzymatic degradation of recalcitrant polysaccharides. *FEBS J.,* 280**,** 3028-3049.

VAAJE-KOLSTAD, G., HORN, S. J., VAN AALTEN, D. M., SYNSTAD, B. & EIJSINK, V. G. H. 2005a. The non-catalytic chitin-binding protein CBP21 from Serratia marcescens is essential for chitin degradation. *J. Biol. Chem.,* 280**,** 28492-28497.

VAAJE-KOLSTAD, G., HOUSTON, D. R., RIEMEN, A. H., EIJSINK, V. G. & VAN AALTEN, D. M. 2005b. Crystal structure and binding properties of the *Serratia marcescens* chitin-binding protein CBP21. *J. Biol. Chem.,* 280**,** 11313-11319.

VAAJE-KOLSTAD, G., WESTERENG, B., HORN, S. J., LIU, Z., ZHAI, H., SØRLIE, M. & EIJSINK, V. G. H. 2010. An oxidative enzyme boosting the enzymatic conversion of recalcitrant polysaccharides. *Science,* 330**,** 219-222.

ZAKARIASSEN, H., EIJSINK, V. G. H. & SØRLIE, M. 2010. Signatures of activation parameters reveal substrate-dependent rate determining steps in polysaccharide turnover by a family 18 chitinase. *Carbohyd.Polym.,* 81**,** 14-20.

ZAKARIASSEN, H., AAM, B. B., HORN, S. J., VÅRUM, K. M., SØRLIE, M. & EIJSINK, V. G. H. 2009. Aromatic Residues in the Catalytic Center of Chitinase A from *Serratia Marcescens* affect Processivity, Enzyme Activity, and Biomass Converting Efficiency. *J. Biol. Chem.,* 284**,** 10610-10617.

Table 1. Primes used for site-directed mutagenesis

Enzyme	Primer	Sequence
ChiB-F190A	forward	5’GCCGGCGGCGCCGCCTTCCTGTCGCG’3
	reverse	5’CGCGACAGGAAGGCGGCGCCGCCGGC’3
ChiB-F190A/W220A	forward	5'-TGGCCGGCCCCGCGGAGAAG-3'
	reverse	5'-CTTCTCCGCGGGGCCGGCCA-3'

Table 2.

Enzyme	*A*	*b*	P^{app}, [a]	P^{app}, [b]
		*Sm*ChiA		
WT	0.32 ± 0.06	0.65 ± 0.13	30.1[c]	36[d]
W167A*[e]	0.05 ± 0.02	0.90 ± 0.25	*n.a.*[f]	16[d]
W275A*	0.06 ± 0.02	0.62 ± 0.21	*n.a.*[f]	14[d]
		*Sm*ChiA with *Sm*LPMO10A		
WT	2.29 ± 0.28	0.51 ± 0.08		
W167A	1.51 ± 0.08	0.38 ± 0.04		
W275A	1.09 ± 0.14	0.75 ± 0.07		
		*Sm*ChiB		
WT	0.31 ± 0.04	0.73 ± 0.1	24.3[c]	*n.d.*[g]
W97A*	0.05 ± 0.01	0.96 ± 0.1	11.0[c]	*n.d.*[g]
W220A*	0.04 ± 0.01	1.16 ± 0.2	9.8[h]	*n.d.*[g]
W97A/W220A	0.06 ± 0.01	0.54 ± 0.1	*n.d.*[g]	*n.d.*[g]
F190A	0.06 ± 0.01	0.84 ± 0.1	11.6[h]	*n.d.*[g]
F190A/W220A	0.04 ± 0.01	0.78 ± 0.1	*n.d.*[g]	*n.d.*[g]
		*Sm*ChiB with *Sm*LPMO10A		
WT	4.16 ± 0.31	0.45 ± 0.05		
W97A	2.71 ± 0.23	0.40 ± 0.06		
W220A	6.48 ± 0.74	0.30 ± 0.08		
W97A/W220A	4.43 ± 0.33	0.23 ± 0.10		
F190A	4.06 ± 0.60	0.54 ± 0.09		
F190A/W220A	4.46 ± 0.20	0.37 ± 0.03		

[a] As determined on the basis of the $[(GlcNAc)_2]/[GlcNAc]$ product ratio during the initial phase of degradation of β-chitin (Hamre et al., 2014).

[b] As determined from the plot of the concentration of enzyme-generated reducing groups *versus* insoluble reducing groups upon chitin degradation under single-hit conditions (Kurašin et al., 2015).

[c] Values obtained from Hamre *et al*. (Hamre et al., 2014).

[d] Values obtained from Kurašin *et al*. (Kurašin et al., 2015).

[e] For mutants marked with a *, the loss of processivity has also been shown in experiments with chitosan; Se Horn *et al*. and Zakariassen *et al*. for more details (Horn et al., 2006, Zakariassen et al., 2009).

[f] Not applicable. An assumption for the use of the $[(GlcNAc)_2]/[GlcNAc]$ product ratio upon degradation of β-chitin is that there should not be a significant different probability of endo-mode initiation between enzymes nor too high degree of endo-mode initiation. Since ChiA-W167A and ChiB-W275A display a high degree of endo-mode initiation that differs significantly from the wild type (Kurašin et al., 2015), this method is not used to assess P^{app}.

[g] Not determined.

[h] Determined in this work.

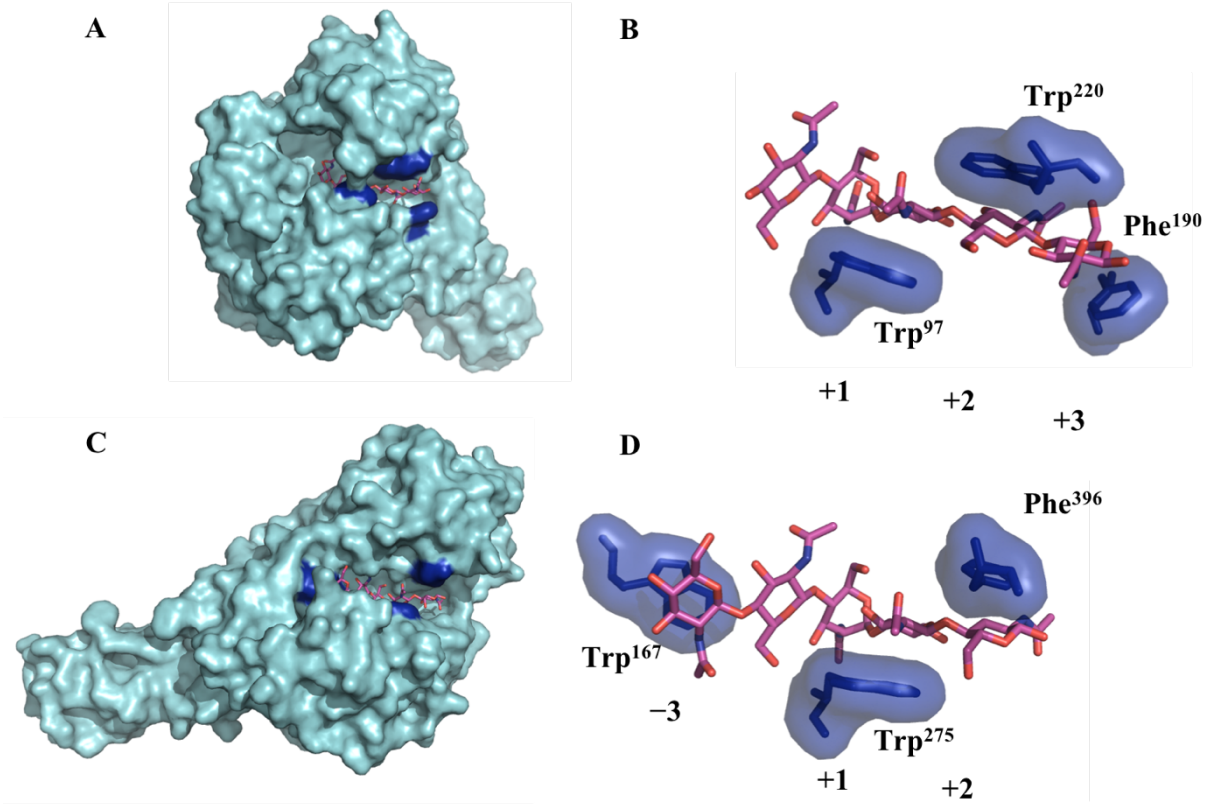

Figure 1. Substrate binding in *Sm*ChiA and *Sm*ChiB. The panels show structurally aligned crystal structures of *Sm*ChiB (A&B; pdb 1e6n (van Aalten et al., 2001)) and *Sm*ChiA (C&D; pdb 1ehn, (Papanikolau et al., 2001)) with substrates. Selected surface exposed aromatic amino acids are highlighted in blue.

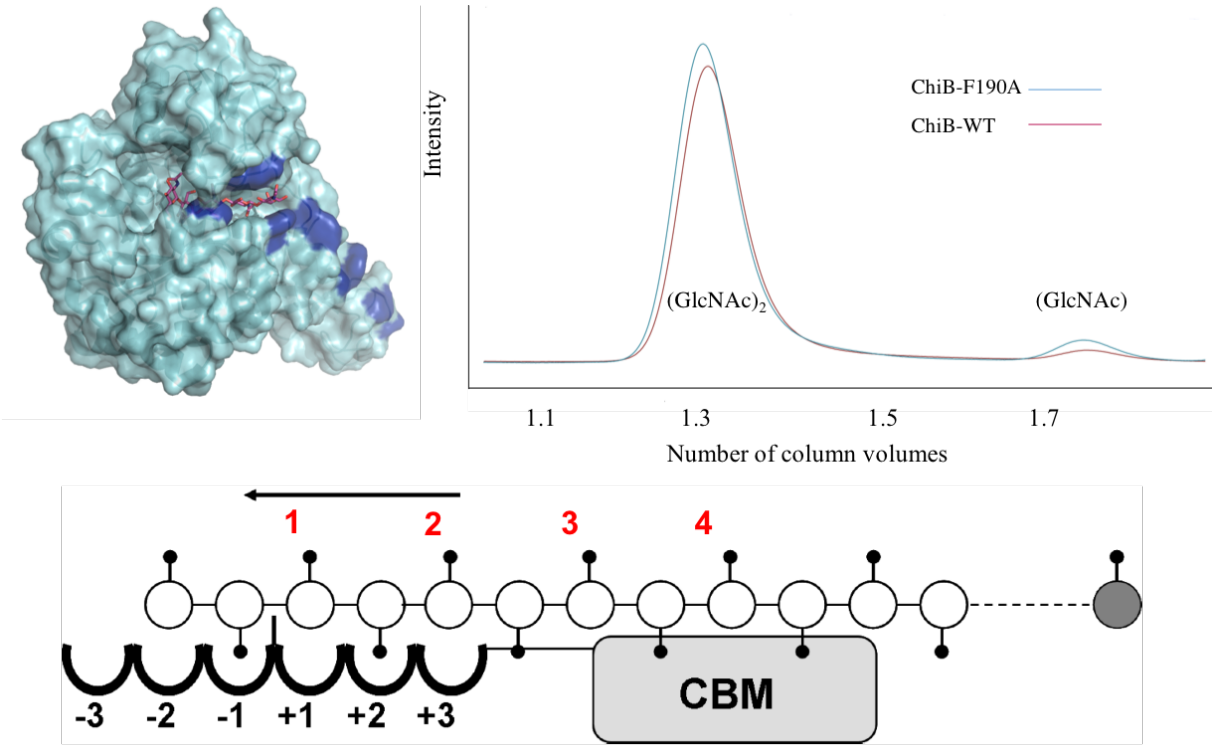

Figure 2. Crystal structure of *Sm*ChiB (top left) and a schematic picture of *Sm*ChiB in complex with a single chitin chain (bottom). Surface exposed aromatic amino acids stacking with sugar moieties (being individual subsites) are highlighted in blue. The glycosidic bond between the sugar residues in subsite –1 and +1 is enzymatically cleaved. A correctly positioned *N*-acetyl group (shown as sticks) in the –1 subsite is essential for the substrate-assisted catalysis. Due to that the smallest structural unit of chitin is a disaccharide, the product of repeated processive enzymatic actions will be dimers, $(GlcNAc)_2$. Monomers, GlcNAc, originate from initial productive binding when the sugar in the non-reducing end occupies a subsite with an odd number. Hence, a high ratio of $[(GlcNAc)_2]/[GlcNAc]$ indicates a high degree of apparent processivity. A chromatogram (top right) of $(GlcNAc)_2$ and GlcNAc resulting from chitin degradation (4 %) is shown for *Sm*ChiB-F190A (red line) and compared to that of *Sm*ChiB-WT (blue line). *Sm*ChiA-F190A is less processive (P^{app} = 11.6) than *Sm*ChiB-WT (P^{app} = 24.3) thus producing higher concentrations of GlcNAc than the wild type.

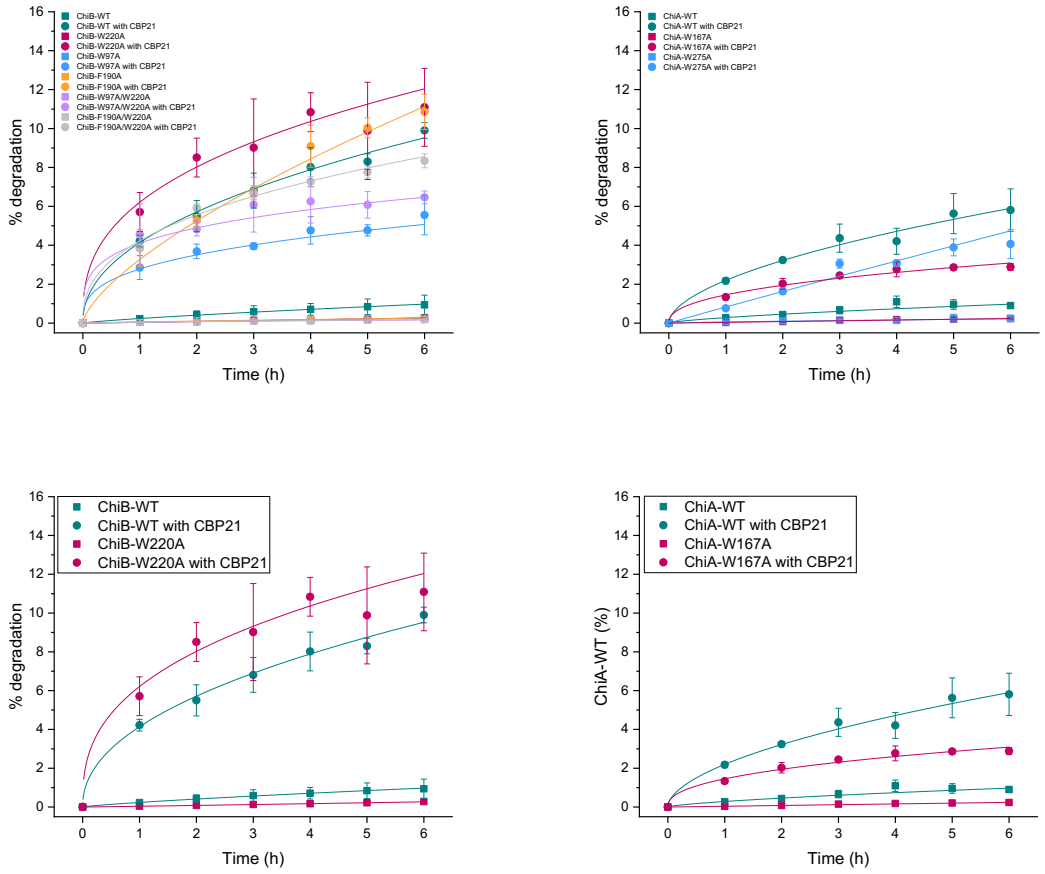

Figure 3. Examples of progress curves fitted to Eq. 1. The top left panel shows data for *Sm*ChiB-WT (green), *Sm*ChiB-W220A (red), *Sm*ChiB-W97A (blue), *Sm*ChiB-F190A (orange), *Sm*ChiB-W97A/W220A (violet), and *Sm*ChiB-F190A/W220A (grey), with (circle) and without (square) *Sm*LPMO10A. The top right panel shows data for *Sm*ChiA-WT (green), *Sm*ChiB-W167A (red), and *Sm*ChiA-W275A (blue), with (circle) and without (square) *Sm*LPMO10A. The hydrolysis were performed with 100 nM enzyme in 50 mM sodium acetate pH 6.1 at 37 °C with 20 mg/ml chitin. The bottom left and right panels focus on the wild types of *Sm*ChiB and *Sm*ChiA, respectively, and the most active mutants, *Sm*ChiB-W220A and *Sm*ChiA-W167A.